Radargrammetric Extraction of Building Features from high resolution multi-aspect SAR Data

U. Soergel[1], E. Michaelsen[2], A. Thiele[2], U. Thoennessen[2]
[1]Institute of Photogrammetry and GeoInformation, University of Hannover, Germany
[2]FGAN-FOM Research Institute for Optronics and Pattern Recognition, D-76275 Ettlingen, Germany
E-mail: soergel@ipi.uni-hannover.de

***Abstract*— State-of-the-art airborne SAR sensors provide spatial resolution on the order of one decimeter. In such data, many features of urban objects are observable, which were beyond the scope of radar remote sensing before. In this paper, the impact of high-resolution SAR data on the analysis of urban scenes is discussed. The new quality of the appearance of buildings in high-resolution data is discussed with a couple of amplitude SAR images taken from orthogonal viewing directions. The fine level of detail opens the opportunity to reconstruct the structure of man-made objects (e.g. buildings). A concept for the radargrammetric building analysis from high-resolution amplitude SAR imagery is proposed and results are presented.**

Keywords-SAR; reconstructuíon; distortion; fusion; urban

I. INTRODUCTION

In general, topographic mapping of urban areas is based on sensor data acquired from airborne platforms in nadir view under good weather conditions, e.g. aerial imagery and LIDAR. An alternative part of the frequency spectrum is the radar domain. Synthetic aperture radar (SAR) sensors provide two-dimensional mapping of the scene. However, the SAR principle requires oblique and side-looking illumination [8]. Consequently, occlusions and multi-bounce signal propagation occur frequently in urban areas [1]. Additionally, layover inevitably takes place at buildings. These effects burden radargrammetic analysis of urban scenes [6] (e.g. SAR stereoscopy). Even in the case of similar viewing aspects, strong dissimilarity of images may occur, leading to a lack of suitable tie points. For this reason radargrammetric stereo has recently been approached on datasets with parallel trajectory and viewing direction but differing in depression angle [9].

Commercial airborne SAR sensors typically provide data of spatial resolution on the order of one meter and upcoming space-borne systems will achieve similar values [7]. First results of experimental airborne SAR systems have shown that even objects in the decimeter scale can be resolved [3]. In such data many features of urban objects are observable, which were beyond the scope of radar remote sensing before. This seems to offer the opportunity to overcome some limitations of building recognition from SAR data in dense urban areas [5][10].

Examples for the new quality of the appearance of buildings in data of decimeter resolution are given and interpreted in Section 2, using two SAR images taken from orthogonal viewing directions.

The signal of roof structures such as eaves and ridges or facade elements appear for the first time well contrasted in the SAR imagery. Such features can now be used as tie structures for a radargrammetric analysis of the building geometry. An approach based on concepts of SAR stereoscopy is proposed in Section 4 and first results are given. The recognition is carried out using a production system [11].

II. BUILDING STRUCTURES IN HIGH-RESOLUTION SAR

The appearance of buildings in high-resolution SAR images is discussed using a building of the Karlsruhe University campus (Germany). Fig 1a depicts a SAR image of about one meter resolution [2]. The very same scene was mapped again twice from the same and an orthogonal aspect, this time with the new FGAN sensor PAMIR [3]. The resolution of the sliding-mode multilook image presented in Fig 1b is slightly better than 20cm in range and azimuth (HH polarization, off-nadir angle 55°). The X-band sensor is capable to provide even better resolution, below one decimeter in both directions.

Comparing the two SAR images 1a and 1b taken from same aspect with different resolution, in particular buildings look very different. Only a few scattering events occur and superimpose inside the small resolution cell of high-resolution SAR. Hence, many more building features like edges and point structures become visible, which were averaged with their surrounding background in the past. This leads as well to larger dynamic range of the data in urban scenes.

A second PAMIR image is shown in Fig 1c. This time the illumination direction is from left to right. The image was focused using strip map processing of a subset of the entire sliding mode data, resulting in approximately 40 cm resolution. Comparing the two PAMIR images some linear roof features and salient rows of point scatterers are visible in both images. Because of the orthogonal viewing directions on the other hand many complementing building features can be observed.

An orthophoto of the test scene is shown in Fig 1d. The PAMIR images and the aerial photo have about the same spatial resolution. Many features of the urban objects are visible in both frequency domains, but some appear in the SAR imagery but not in the aerial image and vice versa. Hence, fusion of these complementing information sources for the analysis of urban structures seems to be fruitful. Furthermore, new opportunities for building recognition from SAR data arise from the high level of detail.

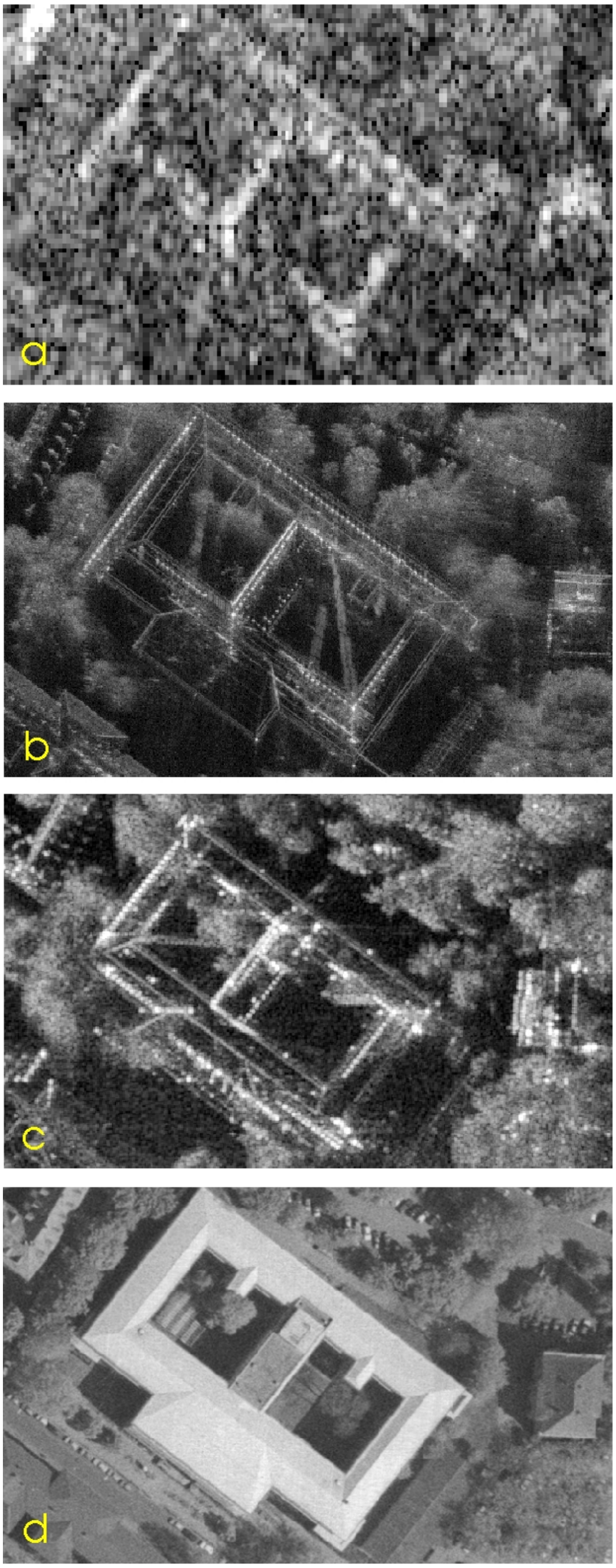

Figure 1. a) AER-II image with one meter resolution (range top-down, b) PAMIR image with resolution better than 20 cm (sliding spotlight mode, range top-down), c) PAMIR image with about 40 cm resolution (illumination from left), d) orthophoto (30cm)

III. Radargrammetric Analysis based on Production System

Traditionally the recognition of the detailed geometric structure of urban areas from remote sensing data was restricted to aerial imagery and LIDAR. Such approaches in general exploit knowledge about frequently observed features of man-made objects such as straight edges, right angles, symmetries and regular or parallel alignment of object groups. Until now, building recognition from SAR suffered mainly from the coarse level of detail of building features in the data [10]. As discussed before, in high-resolution SAR data many of such features became visible, which can now be incorporated into the analysis. Hence, it seems to be worthwhile to adapt existing methods e.g. for building recognition to SAR data. This will be sure a research topic for the next future when more of such data become available.

Here, the potential of such an analysis is demonstrated by the radargrammetric determination of the height of a building based on the matching of salient angle structures of the roof. While the correlation or matching of low-level image structure is pointless due to different illumination, construction of correspondence between higher-level potential building structures makes sense. Furthermore, symmetry axes of buildings are derived. The assembly of more complex objects starting from primitives and the matching process are carried out by a production system. The production net [11] shown in Fig 2 illustrates the workflow.

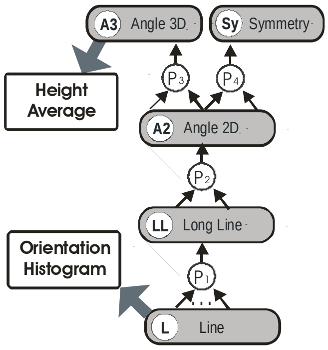

Figure 2. Production net of the system

A. *Pre-processing*

Because only a very limited number of high-resolution SAR data sets are available up to now, no adapted segmentation methods for such imagery are established yet. Instead standard tools were used for the investigations presented in the following. First, in a pre-processing step cropping of small numbers of very strong scatterers and choosing the 40dB of the signal starting from this threshold prune the large dynamic range of the data. Then the signal is mapped to byte format by non-linear operations. Finally, the images are first projected onto ground range and then coregistered.

B. *Feature extraction and production system*

Primitive line objects L are derived using the squared averaged gradient filter [4]. Pixels where the first eigenvalue of this 2x2-Matrix is much bigger than the second one indicate the presence of either an edge or a line at that location. For this example 19.5% of the pixels of the two images have this property. Thus a set of over 100 000 objects *L* is inserted into the system.

From this set of objects *L* long line objects *LL* are built by production P_1. Small gaps between neighbored collinear primitives *L* are bridged in this step. This production first constructs only small prolongations of only several pixels length. But these lead to larger search regions, so that with increasing processing time longer objects *LL* are constructed that may well be several hundred pixels long. The next step is the assembly of 2D angle objects *A2* from adjacent non-collinear objects *LL* with production P_2.

In the search run documented here some 12 500 objects *A2* have been constructed from the primitives that describe the images content sufficiently well after 100 000 search cycles. These are displayed in Fig. 3a as red or green structures depending on the image in which they were found. For better interpretation the building layer from the map is shown as well. The productions P_3 and P_4 used for the feature matching and the search for building symmetries are discussed in the following paragraphs.

C. Feature Matching

Due to the orthogonal illumination, the layover shift is orthogonal, too, which becomes clear by comparing the building footprint with the images. The layover shift l_s of an elevated object depends on its height *h* over the elevation of the ground range plane h_g and the off-nadir angle θ:

$$l_s = h \cdot \cot(\theta)$$

The orthogonal illuminations lead to a straightforward strategy for the search of corresponding structures coded in production P_3. By exploiting geometric constraints it is possible to decide whether two objects *A2* in the different images may result from the same 3D structure. Assuming a certain height of an angle object $A2_L$ produced in the image illuminated from the left results in a shift to the right in the world coordinate system coinciding with the image lines. Analogous, objects $A2_T$ found in the image taken from the top move with rising height downwards along the image column. From matching objects $A2_L$ and $A2_T$ a 3D angle object *A3* is constructed. The constraint resembles that of an epipolar line (going 45^O from lower right to upper left here). It is very restrictive, so that even after 10 000 search cycles with the 12 500 angle objects *A2* only 17 objects *A3* are constructed. Fig. 3b shows that all of them belong to the dominant building in the middle. Fig. 3c gives the histogram of the derived heights in meter. From this a building height of 16.6m is estimated, which is close to the truth. In fact, the eaves of the building are 16 m above ground and the elevation variation of the mayor roof patches of about 2 m is small.

D. Intermediate control decision

The processing effort is concentrated on objects of interest using decisions based on the set of objects inferred so far. The control is capable of preferring objects according to specified attributes or of concentrating on certain sub-systems of the net. In this case an orientation histogram on the objects *L* gives clear hints on the major orientations of the buildings in the processed area. The main effort is on the first stage, where only productions P_1 and P_2 are active. Productions P_3 and P_4 only take about 10% each of the search cycles that are spend on the lower subnet. However, it is clear that at least some of the constructions with the lower net have to be finished before these higher parts can become active.

If production P_3 succeeds in a height estimate it is useful to shift all the objects *A2* according to this. Then production P_4 can construct common symmetry patterns regardless whether the parts stem from one image or the other. Figs. 4a and 4b compare the results of the same search effort with and without such corrections. The following section gives the result.

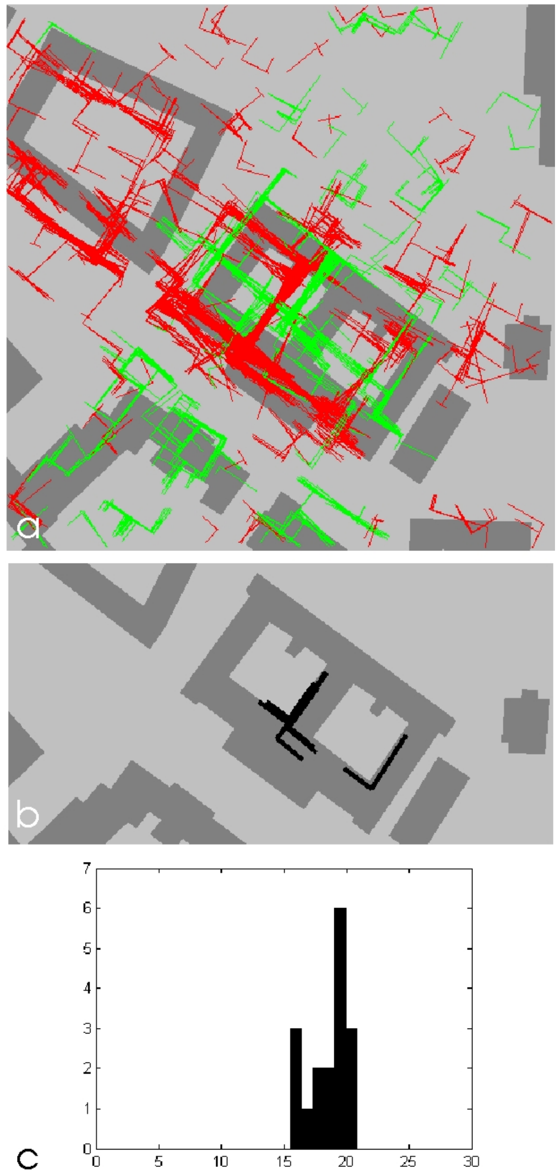

Figure 3. a) angle objects *A2* after 100000 cycles b) 17 3D angle objects *A3*, c) height histogram of objects *A3*.

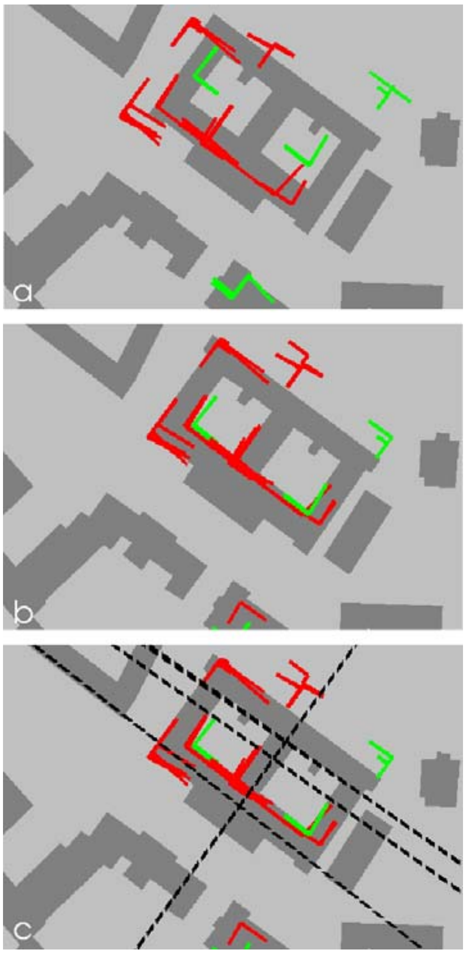

Figure 4. angle objects *A2* used for assembly of symmetry objects *Sy*: a) before, b) after shift, c) like b) plus the detected symmetry axes (black).

E. Detection of Building Symmetry Axes

The symmetry constraint is a non-local constraint and thus fairly weak. Whether on the shifted or original base of angles, production P_4 will come up with some 1200 objects *Sy* after 10000 search cycles. These are assessed according to the degree of their symmetry. Then they are clustered according to their axis. Figs. 4a and 4b display the objects *A2* underlying the clusters of sufficient size and assessment (again using colour code for the image from which they come). Of the 55 objects *A2* remaining in the original version 39 result from structure of the dominant building and 16 are from arbitrary other structures. Compared to this, the shifting leads to 59 objects *A2* where 46 result from structures of the dominant building and 13 from arbitrary other structures. Moreover, the 46 correct objects as well as the two major symmetries of the building are now correctly located in the scene. Symmetry patterns from one image and from the other image are clustered into the same correct axis estimations.

IV. CONCLUSION

State-of-the-art high-resolution SAR sensors provide a detailed mapping of man-made objects, which could not be achieved by radar remote sensing only a few years ago. Structural image analysis approaches were up to now either tailored for extended targets or the extraction of rather coarse scene descriptions. In the new high-resolution data, a much finer level of detail of object features becomes visible. This supports efforts to use radargrammetric methods for the extraction of the structure of urban objects. Especially building recognition approaches from SAR data are expected to yield better results compared to the past, both in terms of accuracy and level of detail. First results based on multi-aspect SAR data presented here are encouraging. Further improvements are expected to be possible from high-resolution InSAR data. The geocoding accuracy should match the resolution of the SAR data and therefore the height reference data must represent the buildings. Precise geocoding is a prerequisite e.g. for the fusion of multi-aspect SAR data or the fusion of SAR data with complementing data of different kind.

ACKNOWLEDGMENT

We want to thank Prof. Dr. Ender and Dr. Brenner (FGAN-FHR Research Institute for High Frequency Physics and Radar Techniques) for providing the SAR data.

REFERENCES

[1] Dong, Y., Forster, B. and Ticehurst, C., 1997. Radar Backscatter Analysis for Urban Environments, Int. Journal of Remote Sensing, Vol. 18, No. 6, pp. 1351-1364.

[2] Ender J.H.G., 1998. Experimental results achieved with the airborne multi-channel SAR system AER-II. Proc. EUSAR'98, pp. 315-318.

[3] Ender, J. H. G. and Brenner, A. R, 2003. PAMIR - a wideband phased array SAR/MTI system. IEE Proceedings - Radar, Sonar, Navigation, vol. 150, no. 3, pp. 165-172.

[4] Foerstner, W. 1994 A Framework for Low Level Feature Extraction. In: J.-O. Eklundh (ed). Computer Vision – ECCV 94, Vol. II, B1, pp. 383-394.

[5] Gamba, P., Houshmand, B., Saccani, M., 2000. Detection and extraction of buildings from interferometric SAR data, IEEE Transactions on Geoscience and Remote Sensing, Vol. 38, No. 1, Part 2, pp. 611 –617.

[6] Leberl, F., 1990. Radargrammetric Image Processing. Artech House, Boston.

[7] Roth, A., 2003. TerraSAR-X: A new perspective for scientific use of high resolution spacebome SAR data, 2nd GRSS/ISPRS Joint Workshop on Remote Sensing and Data Fusion over Urban Areas, URBAN 2003, pp. 22-23.

[8] Schreier, G., 1993. Geometrical properties of SAR images. In G. Schreier (ed.), SAR geocoding: Data and Systems: pp. 103-134. Karlsruhe: Wichmann.

[9] Simonetto, E., Oriot, H., Garello, R., 2003. Radargrammetric Processing for 3-D Building Extraction from High-Resolution Airborne SAR Data. IEEE Int. Geoscience and Remote Sensing Symosium, IGARSS 2003, Toulouse, Vol. 3, pp. 2002-2004.

[10] Soergel, U., Thoennessen, U., Stilla, U., 2003b. Reconstruction of Buildings from Interferometric SAR Data of built-up Areas, in: Ebner H, Heipke C, Mayer H, Pakzad K (eds) Photogrammetric Image Analysis PIA. International Archives of Photogrammetry and Remote Sensing. Vol. 34, Part 3/W8, pp. 59-64.

[11] Stilla, U., Michaelsen, E,. Lütjen, K. 1996. Automatic Extraction of Buildings from Aerial Images, in: F. Leberl, R. Kalliany, M. Gruber (eds.), Mapping Buildings, Roads and other Man-made Structures from Images, IAPR-TC7, Wien, Oldenburg, pp. 229-244.